EXPERIMENTAL SHOCK-LITHIFICATION OF CHONDRITIC POWDER: IMPLICATIONS FOR ORDINARY CHONDRITE REGOLITH BRECCIAS, A. Bischoff, Institute of Mineralogy, Corrensstrasse 24, 4400 Münster, FRG, and M.A. Lange, Alfred-Wegener-Institute for Polar Research, 2850 Bremerhaven, FRG.

Ordinary chondrite regolith breccias show a characteristic light-dark structure. They consist of mineral and lithic clasts of variable sizes bound together to form a tough breccia. Kieffer (1975) suggested that the lithification of fragmental debris to consolidated, tough breccias is caused by impact-induced shock-melting at grain boundaries. Ashworth and Barber (1976) demonstrated that chondrite regolith breccias were affected by shock which resulted in the formation of melted material at grain contacts ("spotted" glass). Bischoff et al. (1982, 1984) studied 14 gas-rich ordinary chondrite regolith breccias to evaluated the nature of the lithification process. They suggested that variable peak shock pressures caused variable amounts of interstitial shock-melted material to transform loose regolith into tough breccias; they found breccias with very low abundances of interstitial melts (class A-breccias) as well as breccias in which subrounded clasts are almost completely surrounded by interstitial, feldspathic materials (class C-breccias). Intermediate breccias exist (class B-breccias).

Bischoff et al. (1984) determined the grain size distribution in the fine-grained (< 150 µm) matrix of the Fayetteville (class A; probably the least shocked and consolidated breccia) ordinary chondrite regolith breccia. Based on these results an equivalent powder from the Forest City H5 chondrite was prepared. All fragments had grain sizes of < 120 µm. The powder was loaded into shock recovery assemblies by use of a specially designed device. In most cases, powders were compacted to the ∿crystal density of the mixture by taking into account the volume of the sample chamber and the appropriate amount of sample material. Some samples were chosen to have various degrees of porosity by decreasing the mass of powder to be compacted (Table 1). The target containers were hung in front of a 20 mm powder gun and were impacted by Lexan projectiles which carried aluminium or stainless steel flyer plates (some projectiles were shot without flyer plates; Table 1). Projectile velocities varied between ∿1 to 1.7 km/sec inducing shock pressures of 4 to 38 GPa via shock wave reverberation. After shock loading, the compacted samples were carefully machined out of the impacted target containers and were used for thin sectioning.

All shock metamorphosed samples were found to be consolidated . However, normal thin section preparation techniques revealed a more pervasive plucking of the lowest-shocked samples compared to higher shocked samples suggesting that these samples are the most poorly consolidated: individual clasts remained discernible in reflected light, whereas samples shocked to 28.0 and 38.2 GPa show locally smooth thin section surfaces suggesting a more intense consolidation.

A Scanning Electron Microscope (SEM) was used to resolve the fine-grained matrix and to get further information on the consolidation process of experimentally shocked samples. The fine-grained matrices vary considerably. SEM observations revealed that the matrices of the samples shocked to pressures as high as 17.4 GPa consist of angular clasts (Fig. 1) locally surrounded by minor amounts of Al-, Na- and Ca-containing, probably feldspathic material, as determined with an energy dispersive analyzer. This effect was nearly independent of sample porosity. These samples are very similar to class A chondrite regolith breccias (Bischoff et al., 1982; 1984). However, those shocked as high as 17.8 GPa with ∿0% sample porosity show a spongy appearance within their fine-grained matrix suggesting a different lithification behaviour compared to the porous samples (Table 1).

The matrix of samples shocked to 28.0 and 38.2 GPa consist of subrounded clasts, that are locally surrounded by higher abundances of shock-melted materials (Fig. 2), and similar to class B- (28.0 GPa) and class C-breccias (38.2 GPa). The interstitial feldspathic material is glassy. Several spots were analyzed by an electron microprobe. Significant loss of Na (!) and K under the electron beam, known from diaplectic glasses (Ostertag, 1981), is documented by relatively low abundances of Na_2O and K_2O (Table 2). SiO_2 is enriched, whereas Al_2O_3 is too low to account for stoichiometric feldspar. CaO is surprisingly high in the interstitial, shock-melted materials compared to typical feldspar of ordinary chondrites (Table 2). We found that the shock-produced, local melt never has a composition of stoichiometric feldspar, excess SiO_2 is obvious. Very similar results were reported by Bischoff et al. (1984) from interstitial melts of the Dimmitt and Nulles (class C) ordinary chondrite regolith breccias: the interstitial melt compositions have high SiO_2- (68.0-76.0 wt.%) and relatively low Al_2O_3- contents (14.8-22.8 wt.%). However, the CaO-contents was usually lower than reported in this study.

EXPERIMENTAL SHOCK-LITHIFICATION

Bischoff, A. and Lange, M.A.

Our observations showed that loose materials are consolidated under shock-pressures as low as 4 GPa. This result confirms the finding of Ahrens and Cole (1974) that regolith fines are compacted at projectile velocities of about 1 km/sec. The formation of interstitial feldspathic material due to shock is responsible to cement and consolidate formerly loose materials. The abundance of interstitial melt is dependent upon the peak shock pressure.

REFERENCES: (1) Ahrens, T.J. and Cole, D.M. (1974), Proc. Lunar Planet. Sci. Conf. 5th, p. 2333-2340. (2 Ashworth, J.R. and Barber, D.J. (1976), Earth Planet. Sci. Lett. 30, p. 222-233. (3) Bischoff, A. et al. (1982), Meteoritics 17, p. 183-184. (4) Bischoff, A. et al. (1984) Earth Planet. Sci. Lett. (in press). Kieffer, S.W. (1975) The Moon 13, p. 301-320. (6) Ostertag, R. (1981), Ph. D. thesis, University of Münster, FRG.

TABLE 1

Shock pressure [GPa]	Porosity %	Projectile (Flyer)	Proj. Velocity [km/sec]	Results
3.9	∿0	Lexan*	1.09	consolidated, clastic, spongy appearence
4.1	17.8	Lexan*	1.04	consolidated, clastic
13.0	∿0	Al	1.05	consolidated, clastic, spongy appearence
13.5	15.0	Al	1.08	consolidated, clastic, minor interstitial melts
17.4	∿0	Al	1.35	consolidated, clastic, minor interstitial melts spongy appearence
28.0	∿0	SS	1.26	consolidated, interstitial glassy melts
38.2	∿0	SS	1.66	consolidated, abundant interstitial glassy melts

* no flyer plate

TABLE 2

	1	2	3	4	5	6	7	8
Na_2O	3.9	1.46	2.10	1.37	1.71	1.79	4.1	9.6
P_2O_5	0.14	0.09	0.20	0.66	0.31	0.23	0.20	n.a.
TiO_2	-	-	0.35	0.18	0.11	0.08	0.19	n.a.
Cr_2O_3	0.05	-	0.15	0.19	-	0.06	-	n.a.
K_2O	1.97	0.68	0.47	0.33	0.81	0.76	0.62	1.00
MgO	0.46	1.58	1.24	4.2	3.5	1.49	-	n.a.
CaO	1.79	3.2	3.8	5.5	3.3	5.5	3.2	2.71
Al_2O_3	20.5	21.0	20.7	19.3	19.8	18.3	21.9	22.1
SiO_2	68.3	69.6	69.0	67.3	69.5	67.0	65.6	64.7
FeO	0.26	0.24	0.71	0.57	0.32	0.58	2.13	0.56
Total	97.37	97.85	98.72	99.60	99.36	95.79	97.94	100.67

Analyses of interstitial melts (1-7) and of a typical plagioclase (8) (Bischoff et al., 1984); n.a.= not analyzed

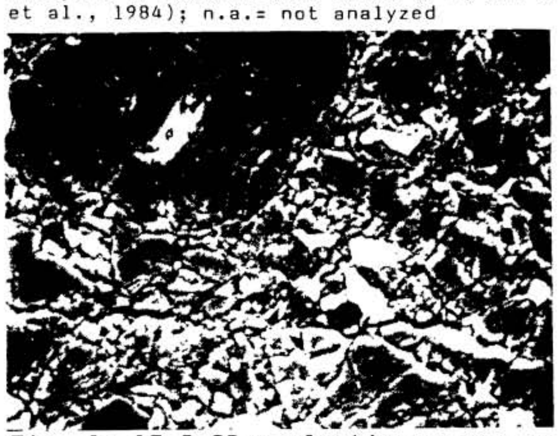

Fig. 1: 13,5 GPa; clastic appearance width: 120 μm

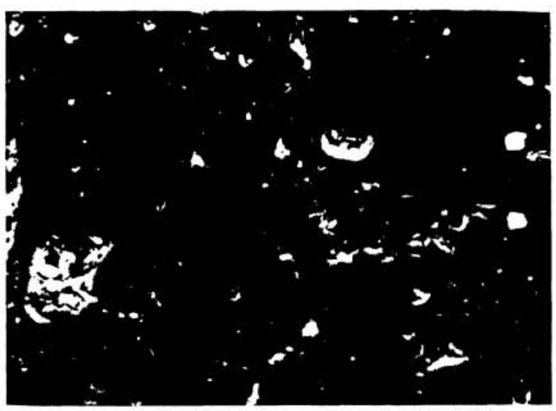

Fig. 2: 38.2 GPa; abundant interstitial glassy melts (dark grey) width: 110 μm